ROTATING FIELD GRADIENT (RFG) MR OFFERS IMPROVED ORIENTATIONAL SENSITIVITY

E. Özarslan[a,b*] *M. Memiç*[a] *A. V. Avram*[c] *M. Afzali*[d†] *P. J. Basser*[c] *C.-F. Westin*[b]

[a]Department of Physics, Boğaziçi University, Bebek, İstanbul, Turkey
[b]Department of Radiology, Brigham & Women's Hospital, Harvard Medical School, Boston, Massachusetts, USA
[c]Section on Tissue Biophysics and Biomimetics, PPITS, NICHD, National Institutes of Health, Bethesda, MD, USA
[d]Department of Electrical Engineering, Sharif University of Technology, Tehran, Iran

ABSTRACT

Rotating field gradients (RFGs), generated by simultaneously applying sine- and cosine-modulated gradient waveforms along two perpendicular directions, provide an alternative diffusion sensitization mechanism for magnetic resonance imaging and spectroscopy. Two RFGs with a 90-degree phase shift between them are applied around the 180-degree RF pulse in a spin echo sequence to measure the diffusion orientation distribution function (dODF) directly. The technique obviates transforming the data from a space reciprocal to the displacement space. Here, we compare RFG results with those obtained by two pulsed field gradient (PFG) techniques: q-ball imaging (QBI) and its extension to constant solid angles (CSA). Our results indicate that RFG provides more accuracy than QBI, while the spurious peaks encountered with the QBI-CSA approach are absent when the RFG-based technique is used. These observations suggest the superior performance of RFG-based methods for mapping the anatomical connections within the nervous system.

Index Terms— MRI, diffusion, anisotropy, connectome, connectivity, tractography, orientation, RFG, rotating, microstructure, white-matter

1. INTRODUCTION

Diffusion-weighted magnetic resonance imaging (MRI) is currently the only noninvasive method that makes it possible to map the orientations of fibrous tissues like muscle and white-matter in the central nervous system. Interest in employing diffusion MRI to map the major connections within the human cerebral network has grown rapidly in recent years. Since the inception of diffusion tensor imaging [1], numerous methods have been introduced to unambigously resolve the underlying fiber orientation(s) [2, 3, 4, 5, 6, 7]. The overwhelming majority of such studies, with the exception of [8], are based on the pulsed field gradient (PFG) experiments featuring a pair of gradient pulses introduced by Stejskal and Tanner in mid 1960s [9]. In this experimental technique, the incorporation of two gradient pulses into a standard pulse sequence sensitizes the signal to diffusion. The MR signal attenuation is then related to the mean apparent propagator, a function that quantifies the likelihood of displacements, through a Fourier relationship.

Most recently, pulse sequences significantly more complicated than the traditional PFG method of Stejskal and Tanner have attracted interest from the community [10, 11, 12, 13, 14, 15, 16]. Among these approaches, rotating field gradient (RFG) MR [13, 14] is the one most relevant for neural connectivity studies.

An RFG "pulse" can be obtained by simultaneously applying two oscillating gradients along perpendicular directions with a 90° phase shift between them. Note that for an RFG pulse, the special direction is the axis of rotation along which sensitivity to diffusion is absent. Furthermore, several such RFG pulses can be employed in succession to design more sophisticated gradient waveforms with potentially interesting properties. For example, two RFG pulses with a 90° phase shift between them (see Figure 1), incorporated into a traditional sequence, lead to rank-2 $\mathbf{b}$-matrices. Several such acquisitions can be performed, each with a different choice for the axis of rotation, and the orientation associated with the maximum signal coincides with that of least hindrance to diffusion. Note that in the case of an orientationally heterogeneous voxel, this effect will be present for all compartments so that the resulting signal profile can be considered to represent the diffusion orientation distribution function (dODF).

In this work, we investigate the RFG response for different levels of diffusion sensitivity (b-values) and compare it

*Support for this work included funding from: (i) TÜBİTAK-EU COFUND Project: 114C015, (ii) Boğaziçi University Research funding BAP 8521, (iii) NIH R01MH074794, and (iv) the Intramural Research Program of the Eunice Kennedy Shriver National Institute of Child Health and Human Development (NICHD), National Institutes of Health (NIH).

†MA performed the work during a visit to Boğaziçi University.

978-1-4799-2374-8/15/$31.00 ©2015 IEEE

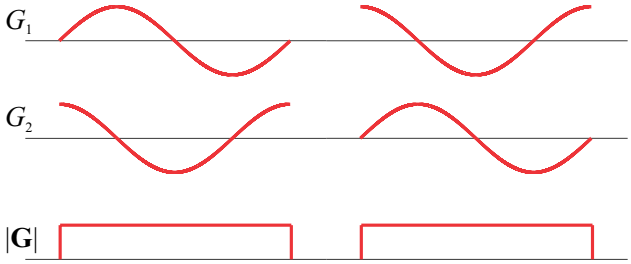

Fig. 1. *First two rows:* An RFG "pulse" involves two oscillating waveforms with a 90° phase shift applied simultaneously along two perpendicular directions. Our sequence involves two such pulses with a 90° phase shift. *Bottom row:* The magnitude profile of the RFG pulse sequence is identical to that of the traditional Stejskal-Tanner pulse sequence.

with PFG-based methods of q-ball imaging (QBI) [2] and its extension to constant solid angles (CSA) [6].

2. THEORY

For the sake of brevity, we shall consider the case in which the rotation takes place on the xy-plane. Suppose that the voxel contains N differently oriented anisotropic, Gaussian compartments with no exchange between them. The signal obtained for this system is given by the expression

$$E(\mathbf{b}) = \sum_{n=1}^{N} [f_n \exp(-\mathbf{b} : \mathbf{D}^{(n)})] , \qquad (1)$$

where f_n is the fraction of the signal for the nth compartment, with the diffusion tensor $\mathbf{D}^{(n)}$, and $\mathbf{b} : \mathbf{D}^{(n)} = b_{ij} D_{ij}^{(n)}$ where Einstein summation convention is employed. Here, b_{ij} is fully determined by the pulse sequence. For the RFG pulse sequence described above,

$$b_{ij} = 4\pi \frac{(\gamma G)^2}{\omega^3} (\delta_{ix}\delta_{jx} + \delta_{iy}\delta_{jy}) , \qquad (2)$$

where γ denotes the gyromagnetic ratio, ω is the angular frequency of rotation, G is the gradient magnitude, and δ is the Kronecker delta. The signal attenuation from this N compartment system is given by

$$E(\mathbf{b}) = \sum_{n=1}^{N} f_n \exp\left[-4\pi \frac{(\gamma G)^2}{\omega^3} \left(D_{xx}^{(n)} + D_{yy}^{(n)}\right)\right] . \qquad (3)$$

Let's examine the contribution of the nth compartment to the expression above. This contribution assumes its maximum value when the rotation takes place along the plane perpendicular to the principal eigenvector of the compartment's diffusion tensor. $E(\mathbf{b})$ is then given by a sum of such contributions weighted by each compartment's signal fraction.

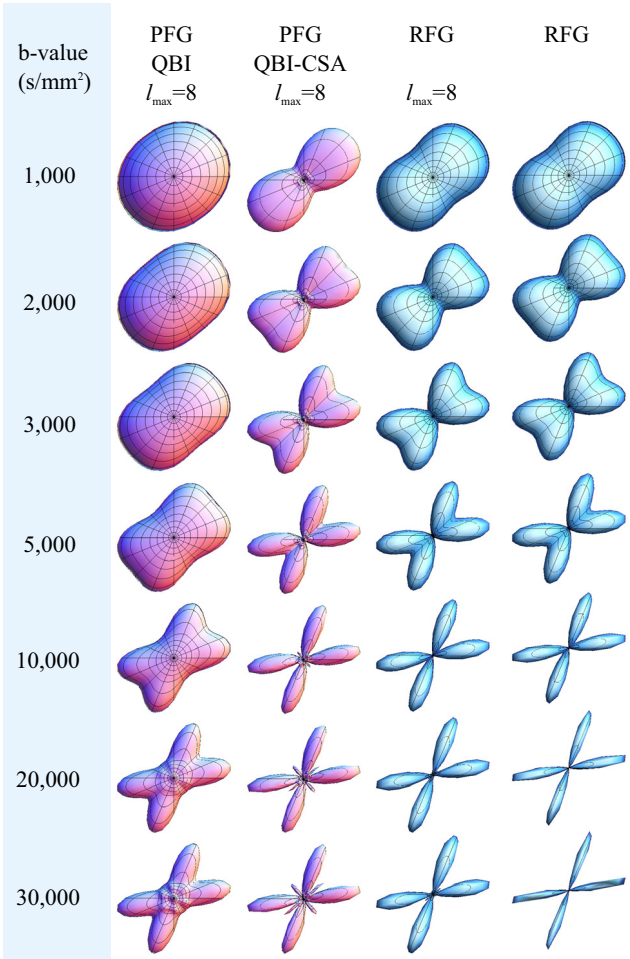

Fig. 2. Diffusion ODFs simulated for a two-compartment system with a 60° crossing angle. Different columns represent different techniques. For the PFG-based methods, we employed the spherical harmonic representation of the dODFs up to a maximum order of $l_{\max} = 8$. To make the comparison meaningful, we also present the same order spherical harmonic representation of the RFG signal though this is not necessary in general. The "raw" RFG signal profiles are shown in the rightmost column.

The above arguments and the associated expressions can easily be generalized to the case of an arbitrary axis of rotation. Such a generalization is necessary as we are primarily interested in protocols that involve repetitions of the scans with many different axes of rotation akin to the high angular resolution diffusion imaging (HARDI) acquisitions [17] for the case of traditional PFG methods.

3. RESULTS AND DISCUSSION

We performed simulations on multi-compartmental systems comprising differently oriented fiber populations. Each com-

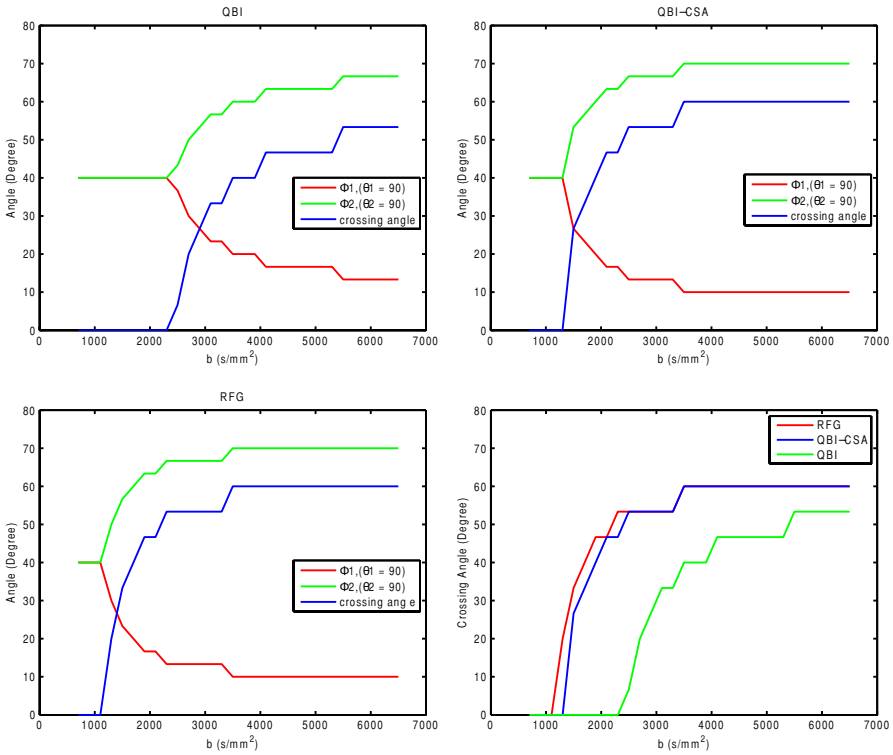

Fig. 3. *First three panels:* The fiber directions (ground truth values: 10° and 70°) and crossing angles (ground truth value: 60°) as estimated by the QBI, QBI-CSA, and RFG methods for different b-values. *Last panel:* Dependence of the estimates of the crossing angle for all three methods plotted against the b-value.

partment was characterized by a diffusion tensor whose trace was taken to be 3×10^{-3} mm2/s, and the eigenvalues had the ratio 10:1:1. To assess the quality of the orientational information provided by the RFG sequence, we focused exclusively on the inherent orientational information without much consideration to acquisition-related concepts such as the signal to noise ratio.

In Figure 2, the simulated dODF profiles for different imaging techniques are shown for various b-values. The PFG-based results are given in the first two columns. In the first case, we show the QBI [2] results obtained using its analytical formulation [5] that employs a series of spherical harmonics up to order $l_{\max} = 8$. This choice for $l_{\max}$ is common in techniques that employ spherical harmonics when sufficient angular resolution is available in the acquired data [4]. The second column represents the same for its CSA-variant [6]. The blue profiles represent the RFG-based results. The rightmost column provides the RFG signal without any manipulation, while the preceding column illustrates its representation in terms of a series of spherical harmonics up to the order $l_{\max} = 8$ for comparison purposes.

Clearly, the response functions get sharper as the b-value is increased. The profiles obtained via QBI suffer from limited angular resolution even in moderate b-values. The sharpness provided by QBI-CSA and RFG methods follow a very similar pattern. However, note that the profiles obtained via the PFG methods suffer from spurious peaks while the RFG signal profiles are virtually free of such artifacts. It should be noted that the sharpness of the profiles revealed by the signal values in the last column could be problematic if the angular resolution is limited. Further, the absence of a representation via spherical harmonics could lead to inaccuracies in the presence of noise.

To quantitate the angular accuracy obtained by the three methods, we computed the peaks of the dODF profiles. The first three panels of Figure 3 show the largest two signal peaks for the PFG-based and RFG methods. The ground truth fiber angles are 10° and 70°, thus the ground truth crossing angle is 60°. Note that QBI doesn't yield the correct values even at b=6,500 s/mm^2. The last panel of this figure includes the estimates of the crossing angle for all three methods. Future work will address the confidence intervals associated with these estimates and assess the sensitivity of the results to diffeent crossing angles.

According to these results in Figures 2 and 3, the best performing technique is RFG followed closely by the CSA method. These observations, lack of spurious peaks in RFG, and the ease with which the technique can be implemented in clinical scanners [14] indicate that RFG MR could be the method of choice in unraveling the complexity of fibrous tis-

sues for connectivity studies.

4. CONCLUSION

The RFG pulse sequence provides one with the ability to measure the dODF directly, obviating the need to transform the signal into a more meaningful function as is done in PFG-based methods. Unlike traditional PFG measurements whose $\mathbf{b}$-matrices are of rank 1, the $\mathbf{b}$-matrix calculated for our sequence has rank 2. As such, diffusion is measured isotropically on the plane of rotation. The QBI technique, in essence, attempts to perform the same operation in the post-processing step by averaging the signal values that reside on a great circle and assigning this average value to the circle's axis. The superior features of the RFG response make it a plausible candidate for next generation connectivity studies. The RFG approach has the potential to offer higher accuracy, fewer artifacts, and removes the dependence of the result on the choice of the estimation technique.

5. REFERENCES

[1] P. J. Basser, J. Mattiello, and D. LeBihan, "Estimation of the effective self-diffusion tensor from the NMR spin echo," *J Magn Reson B*, vol. 103, no. 3, pp. 247–254, 1994.

[2] D. S. Tuch, "Q-ball imaging," *Magn Reson Med*, vol. 52, pp. 1358–1372, 2004.

[3] V. J. Wedeen, P. Hagmann, W.-Y. I. Tseng, T. G. Reese, and R. M. Weisskoff, "Mapping complex tissue architecture with diffusion spectrum magnetic resonance imaging," *Magn Reson Med*, vol. 54, no. 6, pp. 1377–1386, 2005.

[4] E. Özarslan, T. M. Shepherd, B. C. Vemuri, S. J. Blackband, and T. H. Mareci, "Resolution of complex tissue microarchitecture using the diffusion orientation transform (DOT)," *NeuroImage*, vol. 31, no. 3, pp. 1086–1103, 2006.

[5] M. Descoteaux, E. Angelino, S. Fitzgibbons, and R. Deriche, "Regularized, fast, and robust analytical q-ball imaging," *Magn Reson Med*, vol. 58, no. 3, pp. 497–510, 2007.

[6] I. Aganj, C. Lenglet, G. Sapiro, E. Yacoub, K. U. gurbil, and N. Harel, "Reconstruction of the orientation distribution function in single- and multiple-shell q-ball imaging within constant solid angle," *Magn Reson Med*, vol. 64, no. 2, pp. 554–566, 2010.

[7] E. Özarslan, C. G. Koay, T. M. Shepherd, M. E. Komlosh, M. O. Irfanoğlu, C. Pierpaoli, and P. J. Basser, "Mean apparent propagator (MAP) MRI: a novel diffusion imaging method for mapping tissue microstructure," *NeuroImage*, vol. 78, pp. 16–32, 2013.

[8] V. J. Wedeen, G. Dai, W.-Y. I. Tseng, R. Wang, and T. Benner, "Diffusion encoding with 2D gradient trajectories yields natural contrast for 3D fiber orientation," in *Proc. Intl. Soc. Mag. Reson. Med.*, 2006, vol. 14, p. 851.

[9] E. O. Stejskal and J. E. Tanner, "Spin diffusion measurements: Spin echoes in the presence of a time-dependent field gradient," *J Chem Phys*, vol. 42, no. 1, pp. 288–292, 1965.

[10] E. Özarslan and P. J. Basser, "Microscopic anisotropy revealed by NMR double pulsed field gradient experiments with arbitrary timing parameters," *J Chem Phys*, vol. 128, no. 15, pp. 154511, 2008.

[11] J. C. Gore, J. Xu, D. C. Colvin, T. E. Yankeelov, E. C. Parsons, and M. D. Does, "Characterization of tissue structure at varying length scales using temporal diffusion spectroscopy," *NMR Biomed*, vol. 23, no. 7, pp. 745–56, Aug 2010.

[12] S. Eriksson, S. Lasic, and D. Topgaard, "Isotropic diffusion weighting in PGSE NMR by magic-angle spinning of the q-vector," *J Magn Reson*, vol. 226, pp. 13–18, 2013.

[13] E. Özarslan, A. V. Avram, P. J. Basser, and C.-F. Westin, "Rotating field gradient (RFG) MR for direct measurement of the diffusion orientation distribution function (dODF)," in *ISMRM Scientific Workshop on Diffusion as a Probe of Neural Tissue Microstructure*, Podstrana, Croatia, 2013.

[14] A. V. Avram, J. E. Sarlls, P. J. Basser, and E. Özarslan, "Rotating field gradient (RFG) diffusion MRI for mapping 3D orientation distribution functions (ODFs) in the human brain," in *Proc Intl Soc Mag Reson Med*, 2014, vol. 22, p. 4453.

[15] C.-F. Westin, F. Szczepankiewicz, O. Pasternak, E. Özarslan, D. Topgaard, H. Knutsson, and M. Nilsson, "Measurement tensors in diffusion MRI: generalizing the concept of diffusion encoding," *Med Image Comput Comput Assist Interv*, vol. 17, no. 3, pp. 209–216, 2014.

[16] H. Lundell, C. K. Sønderby, and T. B. Dyrby, "Diffusion weighted imaging with circularly polarized oscillating gradients," *Magn Reson Med*, in press.

[17] D. S. Tuch, T. G. Reese, M. R. Wiegell, N. Makris, J. W. Belliveau, and V. J. Wedeen, "High angular resolution diffusion imaging reveals intravoxel white matter fiber heterogeneity," *Magn Reson Med*, vol. 48, no. 4, pp. 577–582, 2002.